

Synthesis and Reactivity of a Dimeric Ni(I) Methyl Complex

Ryan J. Witzke and T. Don Tilley*



Cite This: *Organometallics* 2022, 41, 1565–1571



Read Online

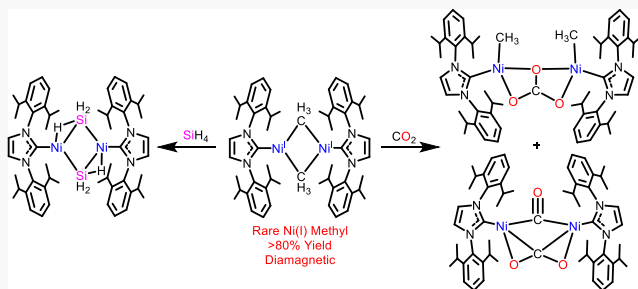
ACCESS |

Metrics & More

Article Recommendations

Supporting Information

ABSTRACT: The synthesis and reactivity of a dimeric Ni(I) methyl complex, $[(\text{IPr})\text{Ni}(\mu\text{-CH}_3)]_2$, (**1**; IPr = 1,3-bis(2,6-diisopropylphenyl)imidazolin-2-ylidene) is reported. Reaction with CO_2 results in the formation of a bridging Ni(II) carbonate species. Additionally, **1** activates a variety of element-H bonds to form methane and new Ni-element linkages. In one instance, treatment with SiH_4 resulted in Si–H bond activation to form a bridging silylene complex, $[(\text{IPr})\text{NiH}(\mu\text{-SiH}_2)]_2$. Finally, complex **1** is a competent catalyst for the coupling of CH_3MgCl with aryl halides.



INTRODUCTION

From the synthesis of the first Ni(I) complex, $\text{K}_4\text{Ni}_2\text{CN}_6$,¹ in 1914 to 2003, only 36 such complexes had been isolated. More recent years have seen a dramatic expansion of the scope and reaction chemistry of Ni(I) complexes, such that now over 280 Ni(I) complexes have been structurally characterized.^{2–4} The recent activity primarily derives from interest in enzymatic active sites and catalytic mechanisms. Active sites in methylcoenzyme M reductase, NiFe-hydrogenase, and acetyl-CoA-synthase/carbon monoxide dehydrogenase contain Ni(I) and catalyze methanogenesis, conversion of dihydrogen to H^+ , and conversion of CO_2 to CO, respectively.^{5–7}

The discovery of Ni(I) in biological systems likely spurred the identification and application of Ni(I) complexes in homogeneous catalysis. While many catalytic reactions are proposed to involve a Ni(0)/Ni(II) cycle, recent investigations suggest that Ni can operate through one electron steps with Ni(I) intermediates.^{8–11} Specifically, the field of Ni-catalyzed Kumada coupling has seen recent reports that corroborate the involvement of Ni(I) species through the isolation of intermediates.^{12–14}

Alkyl complexes of Ni(I) are interesting targets in the context of cross-coupling reactions, as such species have often been implicated in possible catalytic cycles. The Vicic group reported the synthesis of a Ni(I) methyl complex with a terpyridine supporting ligand that catalyzes the cross-coupling of alkyl electrophiles.¹⁵ While this is an interesting system with useful catalytic applications, EPR and computational studies by the same group determined that unpaired spin is delocalized onto the terpyridine ligand, which means that this complex is better described as a Ni(II) compound.¹⁶ More recently, a Ni(I) methyl complex isolated by Diao et al. was found to insert CO_2 .¹⁷

Sigman's dimer, $[(\text{IPr})\text{Ni}(\mu\text{-Cl})]_2$,¹⁸ was identified as a potential starting point for the synthesis of a new Ni(I) methyl

complex. This versatile compound has been used to synthesize a variety of Ni(I) complexes including alkyl, aryl, silyl, and amido species.^{19–21} The current study resulted in discovery of $[(\text{IPr})\text{Ni}(\mu\text{-CH}_3)]_2$ (**1**), which is the subject of stoichiometric and catalytic studies as described below.

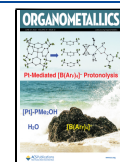
RESULTS AND DISCUSSION

The Ni(I) methyl complex $[(\text{IPr})\text{Ni}(\mu\text{-CH}_3)]_2$ (**1**) was synthesized in 82% yield by a salt metathesis reaction of $[(\text{IPr})\text{Ni}(\mu\text{-Cl})]_2$ with two equivalents of MeMgCl at ambient temperature in Et_2O . The X-ray crystal structure of **1** reveals that the core of the complex consists of a three-center, two-electron bridging methyl ligand with average $\text{Ni}-\text{CH}_3$ and $\text{Ni}-\text{Ni}$ distances of 2.002(11) and 2.310(5) Å, respectively (Figure 1). For comparison, a related Ni(II) complex, $[(\eta^3\text{-dimethylallyl})\text{Ni}(\mu\text{-CH}_3)]_2$, has an average $\text{Ni}-\text{CH}_3$ bond of 2.054 Å and a $\text{Ni}-\text{Ni}$ distance of 2.371 Å.²² Additionally, the $\text{Ni}-\text{Ni}$ distance is shorter than that for metallic Ni (2.39 Å).²³ A structurally similar bridging tolyl complex, $[(\text{IPr})\text{Ni}(\mu\text{-C}_6\text{H}_4\text{CH}_3)]_2$, was recently reported and has similar bond metrics to **1**, with $\text{Ni}-\text{tolyl}$ and $\text{Ni}-\text{Ni}$ distances of 1.936(3) and 2.407(1) Å, respectively.¹³ Similar to the Ni-tolyl complex, **1** is diamagnetic, presumably as a result of antiferromagnetic coupling between unpaired electrons on the Ni centers. A resonance for the bridging $-\text{CH}_3$ groups is located at -2.30 ppm in the ^1H NMR spectrum.

To further probe the electronic state of **1**, density functional theory (DFT) studies were undertaken at the PBE0-D3/def2-

Received: April 18, 2022

Published: June 14, 2022



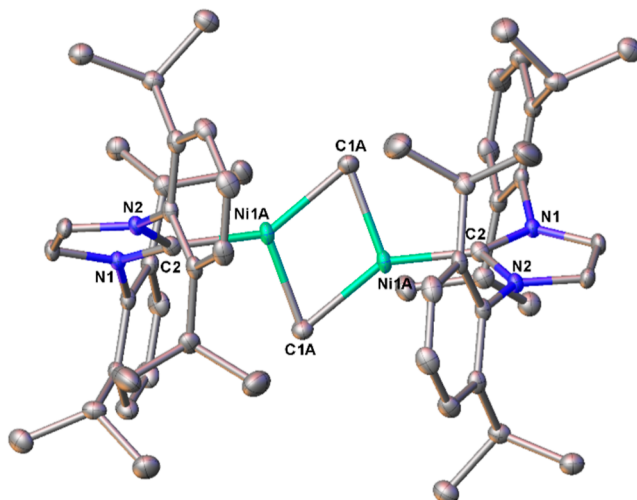


Figure 1. Solid state structure of **1** shown with thermal ellipsoids at 50% probability. A disordered Ni–Me core and all hydrogens were omitted for clarity.

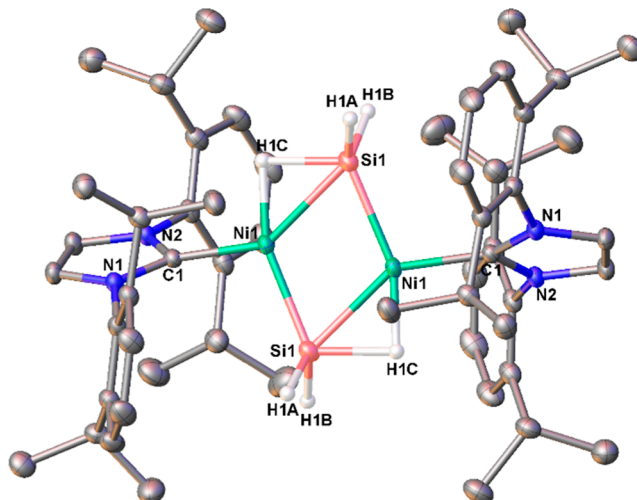
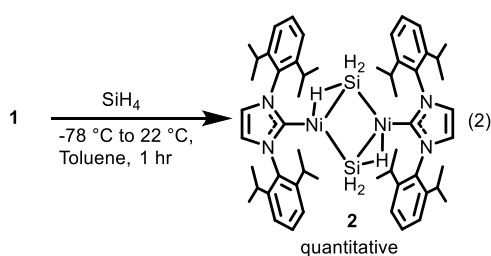


Figure 2. Solid state structure of **2** shown with thermal ellipsoids at 50% probability. A disordered Ni–Si core and all hydrogens (excluding Si–H's) were omitted for clarity. The Si-based hydrogens were located in the electron difference map.



TZVP level of theory for Ni and the atoms directly bonded to Ni, while def2-svpp was used for all other atoms. The optimization was performed by splitting the complex into two $(iPr)_2NiCH_3$ fragments with opposite unpaired spins localized on each Ni. The optimized structure reproduces the X-ray structure of **1** with slight changes to the methyl ligands, which indicates the possibility of an α -agostic C–H interaction with Ni. However, low temperature 1H NMR ($-33\text{ }^\circ\text{C}$) experiments do not provide any evidence for such an interaction. The placement and stabilization of opposite unpaired spins on each Ni fragment is consistent with diamagnetism resulting from antiferromagnetic coupling.

An analogous– SiH_3 complex was targeted for comparison and to assess the ability of the Ni(I) methyl complex to activate Si–H bonds. The high bond dissociation energy of methane ($104.8\text{ kcal mol}^{-1}$) relative to that of SiH_4 ($90.3\text{ kcal mol}^{-1}$)²⁴ suggested that Si–H activation of SiH_4 to form CH_4 and a new Ni complex might be possible. Treatment of **1** in benzene- d_6 with excess SiH_4 resulted in quantitative formation of the red complex $[(iPr)_2Ni(\mu,\eta^2-\text{SiH}_3)]_2$ (**2**), along with CH_4 (by 1H NMR spectroscopy, eq 2). X-ray quality crystals were



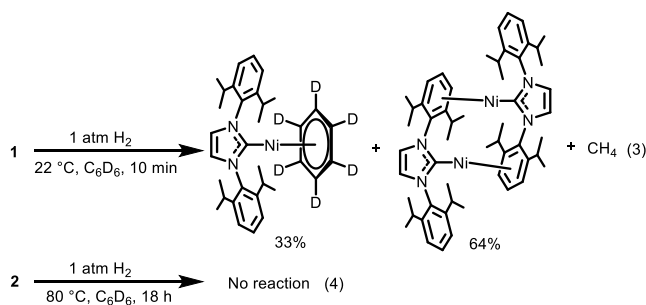
grown from a concentrated toluene solution layered with pentane. The solid-state structure (Figure 2) contains the silyl

complex as a dimer similar to **1**, with bridging $-\text{SiH}_3$ ligands. The Ni–Ni distance is $2.493(1)\text{ \AA}$, which is about 0.2 \AA longer than that of **1**. Also, location of the Si-based hydrogens in the electron difference map revealed strong activation of a Si–H bond at each Ni center, significantly toward a μ - SiH_2 hydride structure. The Ni–Si distances are therefore inequivalent, at $2.253(1)\text{ [Ni}(\eta^2\text{-H})\text{Si] and }2.193(1)\text{ \AA}$. The closest structural analogue to **2** is the recently reported complex $[(iPr)_2Ni(\mu,\eta^2-\text{SiHPh}_2)]_2$, which has similar Ni–Si distances of $2.258(1)$ and $2.200(1)\text{ \AA}$.²⁰ Compared to monomeric Ni(I) silyl complexes, such as $(dtbpe)_2Ni-\text{SiHMe}_2$ [$2.373(1)\text{ \AA}$]²⁵ and $(iPr)_2Ni-\text{Si}(\text{SiMe}_3)_3$ [$2.283(1)\text{ \AA}$],²⁰ **2** possesses shorter Ni–Si distances. Additionally, **2** has longer Ni–Si distances than Ni complexes with silylene character, such as $[(dtbpe)_2Ni(\mu\text{-H})\text{SiMes}_2][\text{BAr}^F_{24}]$ [$2.147(2)\text{ \AA}$]²⁵ and $[\text{PhB}(\text{CH}_2\text{PPh}_2)_3\text{Co}(\mu\text{-H})\text{SiMes}_2$ [$2.142(1)\text{ \AA}$].²⁶

At room temperature, the $-\text{SiH}_3$ resonance in the 1H NMR spectrum is too broad to identify, but decoalescence into two distinct resonances at low temperature ($-60\text{ }^\circ\text{C}$, toluene- d_8) allowed for identification of Ni–H and SiH_2 resonances at -3.30 ppm ($^1J_{\text{SiH}} = 23\text{ Hz}$, 1H) and 4.43 ppm ($^1J_{\text{SiH}} = 163\text{ Hz}$, 2H), respectively. The ^{29}Si chemical shift of 50.8 ppm is most consistent with a silyl ligand.²⁷ The low Si–H coupling constant associated with the nickel hydride resonance is consistent with a weak Si–H interaction.

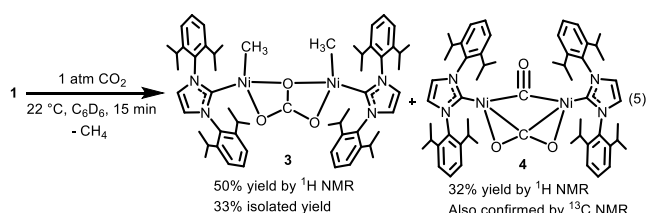
Complex **2** is significantly more thermally stable relative to **1**. Heating **1** to $75\text{ }^\circ\text{C}$ for 1 h in benzene- d_6 resulted in reductive elimination of ethane and formation of a mixture of $[(iPr)_2Ni]_2$ and $(iPr)_2Ni(\eta^6-\text{C}_6\text{D}_6)$,²⁸ whereas **2** was heated to $85\text{ }^\circ\text{C}$ for 4 days in benzene- d_6 with no observable decomposition. The bridging Ni–H–Si hydrides likely play a role in the stabilization of this complex, as such an interaction should inhibit the elimination of H_3SiSiH_3 . Additionally, the Si–Si bond in H_3SiSiH_3 is weaker than the C–C bond in ethane by 14 kcal mol^{-1} , reducing the driving force for elimination.²⁴

To synthesize a bridging hydride complex, **1** was treated with 1 atm of H_2 (in benzene- d_6). This resulted in reduction to $[(iPr)_2Ni]_2$ (64% yield) and $(iPr)_2Ni(\eta^6-\text{C}_6\text{D}_6)$ (33% yield) along with formation of CH_4 (eq 3). A similar result was



encountered by Sadighi et al. in their attempts to synthesize a Ni(I) hydride from $[(\text{IPr})\text{Ni}(\mu\text{-Cl})]_2$ using either $\text{Li}(\text{HBET}_3)$ or $\text{NaO}^{\text{t-Bu}}/\text{HSi}(\text{OEt})_3$ as the hydride source.²⁸ It is likely that the putative hydride product quickly releases H_2 to form the resulting Ni(0) products. Interestingly, treatment of the silyl complex **2** with 1 atm of H_2 resulted in no reaction (in benzene- d_6 at 80 °C, over 18 h) by ^1H NMR spectroscopy (eq 4).

The insertion of CO_2 into the Ni–CH₃ bond of (*t*BuXantphos)Ni(CH₃)¹⁷ mentioned above, to form a Ni(I) carboxylate is of particular interest given the synthetic and catalytic implications for utilization of an abundant and ecologically relevant C₁ source.^{29,30} Treatment of **1** with 1 atm of CO_2 resulted in oxidation to an unusual Ni(II) carbonate species, $[(\text{IPr})\text{Ni}(\text{CH}_3)]_2(\mu\text{-}\kappa^2\text{-CO}_3)$ (**3**), instead of the expected product of insertion, (*IPr*)Ni(O₂CCH₃) (eq 5).



The solid-state structure, shown in Figure 3, reveals a distorted square planar geometry about the Ni centers. The independent Ni–CH₃ distances of 1.895(1) and 1.905(1) Å are shorter than those found in **1**, presumably due to their terminal nature and the higher oxidation state for Ni. The CO₃²⁻ C–O bond distances are 1.331(1), 1.264(1), and 1.265(1) Å, with the longest distance corresponding to the oxygen atom that

bridges the two Ni atoms. Though **3** is diamagnetic, the resonances corresponding to half of the *IPr* *iso*-propyl groups and the –CH₃ ligand are broad at 22 °C in the ^1H NMR spectrum. Additionally, the number of resonances correspond to a C_{2v} symmetric structure instead of the isomer shown in Figure 3. When the temperature was lowered to –53 °C (in toluene- d_8), the resonances sharpened, and two geometric isomers of **3** became observable. One is shown in Figure 3, and the other (with C_{2v} symmetry) is shown in eq 5.

There is precedent for Ni-mediated reductive disproportionation of CO₂ to form CO and CO₃²⁻.^{31–33} Specifically, a Ni(I) complex supported by a β -diketiminate ligand was shown to react with CO₂ to form a Ni carbonate species and free CO.³³ Monitoring the reaction of eq 5 by ^1H NMR spectroscopy showed that **3** formed in approximately 50% yield. The corresponding CO-containing product was found to be $[(\text{IPr})\text{Ni}]_2(\mu\text{-CO})(\mu\text{-}\eta^2\text{-CO}_2)$ ²⁸ (**4**), observed in 32% yield by ^1H NMR spectroscopy. A resonance for methane was also present in the ^1H NMR spectrum of the crude reaction mixture. To further investigate the reduction of **1** to **4**, the reaction of **1** with CO was investigated. Treatment of **1** with 1 atm of CO resulted in the immediate formation of (*IPr*)Ni(CO)₃³⁴ in 73% yield along with the formation of ethane, by ^1H NMR spectroscopy. Similar to the reaction between **1** and CO₂, this addition also involves reduction to a Ni(0) complex. It then seems plausible that the reaction of eq 3 involves reduction of **1** by CO to form a Ni(0) complex, which is then trapped by CO₂ to generate **4**. Related to these reactions, treatment of **2** with 1 atm of CO also resulted in formation of (*IPr*)Ni(CO)₃ by ^1H NMR spectroscopy.

Because complex **3** retains its –CH₃ ligands, it is unlikely that these groups are involved in facilitating **1**'s reaction with CO₂, and this result suggests that the Ni(I) precursor to **1**, $[(\text{IPr})\text{Ni}(\mu\text{-Cl})]_2$, should exhibit similar reactivity. Thus, $[(\text{IPr})\text{Ni}(\mu\text{-Cl})]_2$ was treated with an atmosphere of CO₂, but no reaction was observed after 18 h in benzene- d_6 and 22 °C. This result suggests that the electronic properties of the –CH₃ ancillary ligand are responsible for effecting the CO₂ activation by **1**. Interestingly, treatment of **2** with 1 atm of CO₂ resulted in no reaction by ^1H NMR spectroscopy, even upon heating to 70 °C for 2 h. The reactivity of **1** and **2** toward CO₂ contrasts with that previously observed for the Ni(I) alkyl and silyl complexes (*IPr*)NiC(SiMe₃)₃ and (*IPr*)NiSi(SiMe₃)₃.²⁰ In

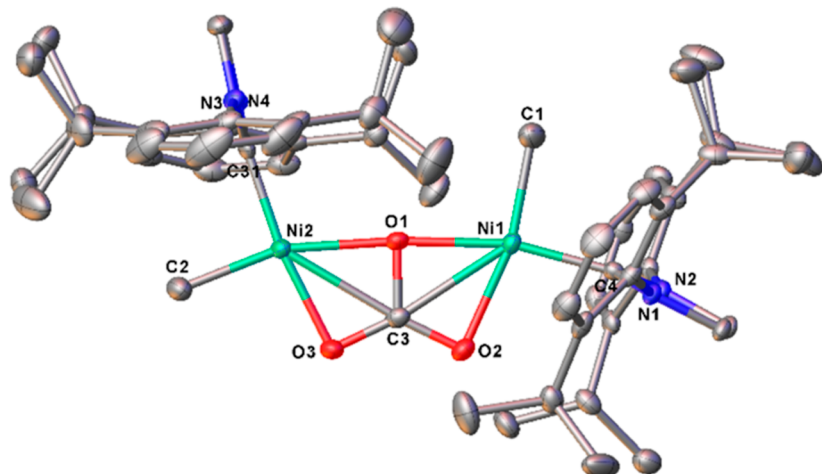
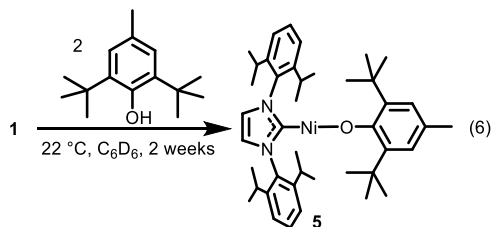


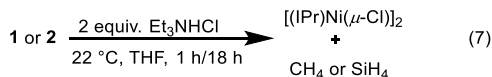
Figure 3. Solid state structure of **3** shown with thermal ellipsoids at 50% probability. All hydrogens were omitted for clarity.

the latter system, the Ni alkyl complex was observed to be inert toward CO_2 , while the analogous silyl complex undergoes insertion of CO_2 to form a silylcarboxylate species.

Treatment of **1** with 2,6-di-*tert*-butyl-4-methylphenol (BHT) over 2 weeks at 22 °C resulted in formation of the previously reported, two-coordinate phenoxy complex **5** (eq 6).³⁵ Treatment of **2** with BHT resulted in no reaction after 18 h at 70 °C in benzene-*d*₆.



Treatment of complex **1** with excess H_2O in tetrahydrofuran (THF) at 22 °C for 6 h resulted in formation of a complex mixture of products; however, **2** is persistent in the $\text{H}_2\text{O}/\text{THF}$ solution after heating to 70 °C for 24 h. Treatment of **1** and **2**, separately, with two equivalents of Et_3NHCl resulted in formation of $[(\text{IPr})\text{Ni}(\mu\text{-Cl})]_2$ and the corresponding gas (CH_4 or SiH_4) by ¹H NMR spectroscopy (eq 7).



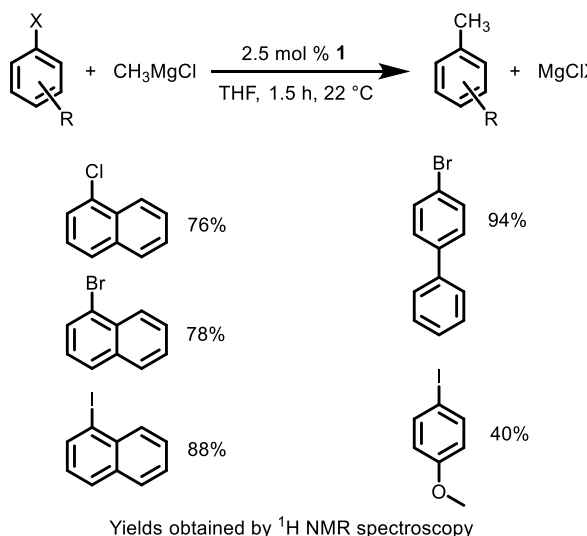
The possible participation of Ni(I) alkyl species in the mechanism of nickel-catalyzed, C–C cross couplings has been a topic of longstanding interest. With respect to N-heterocyclic carbene (NHC) Ni-based catalysts, recent studies have addressed the mechanism of C–C cross-coupling with aryl Grignards and aryl halides using both monometallic and bimetallic Ni(I) complexes.^{13,36} In a study focused on a bimetallic Ni system, the authors conclude that catalysis proceeds through $[(\text{IPr})\text{Ni}(\mu\text{-Cl})]_2$ with a Ni(I/II) catalytic cycle. Due to the nature of **1** as a Ni(I) alkyl complex and its close structural relation to previously reported catalysts, its ability to function as a catalyst for Kumada coupling was investigated.

Complex **1** was treated with two equivalents of iodonaphthalene to yield two equivalents of methylnaphthalene and $[(\text{IPr})\text{Ni}(\mu\text{-I})]_2$ (**6**). The formation of **6** was confirmed by X-ray crystallography and independent synthesis via modification of the procedures used to form $[(\text{IPr})\text{Ni}(\mu\text{-Cl})]_2$ ¹⁸ and $[(\text{IPr})\text{Ni}(\mu\text{-Br})]_2$ ¹⁹ (see Experimental Section). With confirmation that **1** can form C–C bonds in a stoichiometric reaction, use of **1** as a catalyst for coupling CH_3MgCl with a variety of aryl halides was investigated. These reactions resulted in decent yields after only 1.5 h at 22 °C in THF (Scheme 1). Unsurprisingly, moving from Cl^- to Br^- to I^- improves the overall yield of product.

CONCLUSIONS

In summary, this study provides a description of bond activations available to a Ni(I) methyl complex (**1**) and the remarkable stability of a related silyl complex (**2**). Complex **1** promotes the reductive disproportionation of CO_2 to CO_3^{2-} and CO in the form of **3** and **4**, respectively. It is unlikely that a catalytic system can be developed for this transformation, because the formation of CO results in loss of the methyl

Scheme 1. Kumada Coupling of CH_3MgCl and Aryl Halides Catalyzed by **1**



ligands. Complex **1** activates Si–H and O–H bonds to form **2** and **5**, respectively, and it is likely that related bond activations are possible. The difference in reactivity between the methyl (**1**) and silyl (**2**) complexes is quite pronounced, with the only reactions observed for **2** occurring with CO and Et_3NHCl . The stark difference between these two complexes is not entirely unsurprising as late metal silyl species are generally less reactive than analogous alkyl complexes.^{37,38} These results offer new pathways to Ni(I) species with potential for a wide range of structures and functionalities. Additionally, the activity of **1** as a catalyst for Kumada coupling is of particular interest. Future work will focus on the scope, activity, and mechanism of the latter reaction.

EXPERIMENTAL SECTION

General Comments. Unless otherwise noted, all experiments were conducted with dry, oxygen-free solvents using standard Schlenk techniques or VAC Atmosphere or MBRAUN nitrogen-filled gloveboxes. Toluene (ACS grade) and pentane [high-performance liquid chromatography (HPLC) grade] were purchased from Fischer Scientific. Diethyl ether (HPLC grade) was purchased from Honeywell. THF (ChromAR) was purchased from Macron Fine Chemicals. Toluene, pentane, diethyl ether, and THF were dried and deaerated using a JC Meyers Phoenix SDS solvent purification system. Benzene-*d*₆, THF-*d*₈, and toluene-*d*₈ were purchased from Cambridge Isotope Laboratory and dried over 3 Å molecular sieves. The sieves were dried under high vacuum at 250 °C for 2 days. Unless otherwise noted, reagents were obtained from commercial suppliers and used as received. Potassium *tert*-butoxide was purchased from Sigma-Aldrich and sublimed before use. $[(\text{IPr})\text{Ni}(\mu\text{-Cl})]_2$ ¹⁸ was prepared by literature procedure. All ¹H NMR spectra were taken at ambient temperature (ca. 21 °C) on Bruker AV-300, AVB-400, AVQ-400, AV-500, DRX-500, or AV-600 spectrometers each equipped with a 5 mm BB probe and referenced to the residual protio-solvent signals. Solution magnetic susceptibilities were determined by Evans method using ¹H NMR spectroscopy.³⁹ Elemental analyses were conducted by the UC Berkeley College of Chemistry Microanalytical Facility. Single crystal X-ray diffraction experiments for **1**, **2**, **3**, and **6** were performed at beamline 12.2.1 of the Advanced Light Source at Lawrence Berkeley National Laboratory. Frames were collected on a PHOTON II detector running shutterless using radiation with a wavelength of 0.7288 Å selected by a Si(111) monochromator and focused to 200 μm ² with a toroidal mirror. Crystals were kept at 100(2) K throughout collection. Data collection, integration, scaling, and space

group determination were performed with Bruker APEX3 (v. 2016.5-0) software. Structure was solved by SHELXT-2014 and refined with SHELXL-2014, with refinement of F^2 on all data by full-matrix least squares.^{40–42} The three-dimensional molecular structure figures were visualized with Olex2.⁴³

Preparation of $[(\text{IPr})\text{Ni}(\mu\text{-CH}_3)]_2$ (1). To a 20 mL scintillation vial was added 287.5 mg (0.298 mmol) of $[(\text{IPr})\text{Ni}(\mu\text{-Cl})]_2$. The yellow-green solid was dissolved in 6 mL of Et_2O . Then, 0.20 mL of a 3.0 M solution of MeMgCl in THF was added to the stirring solution of Ni, resulting in an immediate color change to brown. The reaction mixture was allowed to stir for 1 h before filtration to remove the salts. The solution was then concentrated and cooled to -35°C for 18 h to form 227.5 mg of brown crystals of $[(\text{IPr})\text{Ni}(\mu\text{-CH}_3)]_2$ (82.6%). ^1H NMR (600.13 MHz, benzene- d_6 , 23 °C): δ 7.24 (t, J = 7.67 Hz, 4H, para-CH), 7.11 (d, J = 7.69 Hz, 8H, meta-CH), 6.53 (s, 4H, NCH), 3.11 (m, J = 6.89 Hz, 8H, $\text{CH}(\text{CH}_3)_2$), 1.31 (d, J = 6.87 Hz, 24H, $\text{CH}(\text{CH}_3)_2$), 1.11 (6.92 Hz, 24H, $\text{CH}(\text{CH}_3)_2$), -2.30 (s, 6H, $\mu\text{-CH}_3$). $^{13}\text{C}\{\text{H}\}$ NMR (150.92 MHz, benzene- d_6): δ 199.74 (carbene C), 146.60 (aryl C), 138.08 (aryl C), 128.83 (para-C), 123.67 (meta-C), 121.80 (NCH), 28.72 ($\text{CH}(\text{CH}_3)_2$), 25.20 ($\text{CH}(\text{CH}_3)_2$), 23.77 ($\text{CH}(\text{CH}_3)_2$), 21.29 ($\mu\text{-CH}_3$). Anal. Calcd for $\text{C}_{56}\text{H}_{78}\text{N}_4\text{Ni}_2$: C, 72.74%; H, 8.50%; N, 6.06%. Found: C, 73.00%; H, 8.34%; N, 6.20%.

Preparation of $[(\text{IPr})\text{Ni}(\mu\text{-SiH}_3)]_2$ (2). To a 250 mL Schlenk flask was added 496 mg (0.536 mmol) of $[(\text{IPr})\text{Ni}(\mu\text{-CH}_3)]_2$. The brown solid was dissolved in 15 mL of toluene to form a dark brown solution. The reaction flask was degassed by freeze–pump–thawing three times. While cooled to -78°C , 1 atm of a 15% SiH_4/N_2 mixture was added to the reaction flask. After the addition, the flask was allowed to stir for 1 h while warming to ambient temperature. Over this time, the reaction solution turned bright orange/red. Then, the solvent was removed under reduced pressure to form a red solid. The crude solid was crystallized from a concentrated solution of toluene layered with pentane, cooled to -35°C for 18 h to obtain 254 mg of 2 (50% yield). ^1H NMR (600.13 MHz, C_6D_6 , 24 °C): δ 7.23 (t, J = 7.70 Hz, 4H, para-CH), 7.09 (d, J = 7.70 Hz, 8H, meta-CH), 6.59 (s, 4H, NCH), 3.02 (m, J = 6.64 Hz, 8H, $\text{CH}(\text{CH}_3)_2$), 1.29 (d, J = 6.70 Hz, 24H, $\text{CH}(\text{CH}_3)_2$), 1.06 (d, J = 6.72 Hz, 24H, $\text{CH}(\text{CH}_3)_2$). ^1H NMR (600.13 MHz, toluene- d_8 , -60°C): δ 7.19 (t, J = 7.57 Hz, 4H, para-CH), 7.00 (d, J = 7.45 Hz, 8H, meta-CH), 6.43 (s, 4H, NCH), 4.48 (s, $^1\text{J}(\text{Si}-\text{H})$ = 162.9 Hz, 4H, SiH_2), 3.00 (m, J = 6.21 Hz, 8H, $\text{CH}(\text{CH}_3)_2$), 1.29 (d, J = 5.95 Hz, 24H, $\text{CH}(\text{CH}_3)_2$), 1.07 (d, J = 6.36 Hz, 24H, $\text{CH}(\text{CH}_3)_2$), -3.30 (s, 2H, Ni–H). $^{13}\text{C}\{\text{H}\}$ NMR (150.92 MHz, C_6D_6 , 25 °C): δ 199.04, 146.32, 137.41, 129.24, 123.90, 122.64, 28.74, 25.60, 23.80. Anal. Calcd for $\text{C}_{54}\text{H}_{78}\text{N}_4\text{Ni}_2\text{Si}_2$: C, 67.79%; H, 8.22%; N, 5.86%. Found: C, 67.89%; H, 8.16%; N, 5.60%.

Preparation of $[(\text{IPr})\text{Ni}(\text{CH}_3)]_2\text{CO}_3$ (3). A 25 mL PTFE-stoppered flask was charged with 86.0 mg (0.0930 mmol) of $[(\text{IPr})\text{Ni}(\mu\text{-CH}_3)]_2$ and 5 mL of Et_2O . The resulting brown solution was then degassed and an atmosphere of CO_2 was added to the flask. An immediate color change to bright orange was observed. The reaction mixture was stirred for 1 h before the excess CO_2 and solvent were removed under vacuum. The crude reaction mixture was then dissolved in minimal Et_2O , and the resulting solution was cooled to -35°C . After 12 h, yellow-orange X-ray quality crystals of $[(\text{IPr})\text{Ni}(\text{Me})]_2\text{CO}_3$ were obtained. Over two crops, a yield of 30.3 mg (33.6%) was achieved. ^1H NMR (400.13 MHz, 22 °C, C_6D_6): δ 7.41 (br s, 4H, para-CH), 7.30 (br s, 8H, meta-CH), 6.42 (s, 4H, NCH), 2.83 (br s, 8H, $\text{CH}(\text{CH}_3)_2$), 1.43 (br s, 24H, $\text{CH}(\text{CH}_3)_2$), 1.02 (d, J = 6.82 Hz, 24H, $\text{CH}(\text{CH}_3)_2$), -0.91 (br s, 6H, Ni–CH₃). ^1H NMR (600.13 MHz, -53°C toluene- d_8) high symmetry isomer δ 7.55 (t, J = 7.61 Hz, 4H, para-CH), 6.92 (d, J = 7.45 Hz, 8H, meta-CH), 6.25 (s, 4H, NCH), 2.41 (m, 8H, $\text{CH}(\text{CH}_3)_2$), 1.51 (d, 24H, $\text{CH}(\text{CH}_3)_2$), 1.44 (d, 24H, $\text{CH}(\text{CH}_3)_2$), -0.92 (s, 6H, Ni–CH₃); low symmetry isomer δ 7.48–7.22 (m, 12H), 6.39 (s, 2H), 6.16 (s, 2H), 3.27 (m, 4H, $\text{CH}(\text{CH}_3)_2$), 1.87 (m, 2H, $\text{CH}(\text{CH}_3)_2$), 1.75 (d, 6H, $\text{CH}(\text{CH}_3)_2$), 1.73 (m, 2H, $\text{CH}(\text{CH}_3)_2$), 1.14–0.96 (m, 36H, $\text{CH}(\text{CH}_3)_2$), 0.88 (d, 6H, $\text{CH}(\text{CH}_3)_2$), -0.66 (s, 3H, Ni–CH₃), -1.09 (s, 3H, Ni–CH₃). ^{13}C NMR (150.92 MHz, 22 °C, benzene- d_6): δ 146.86, 136.60, 130.11, 124.36, 65.95, 28.73, 26.18, 23.17,

15.63. Anal. Calcd for $\text{C}_{57}\text{H}_{78}\text{N}_4\text{O}_3\text{Ni}_2$: C, 69.53%; H, 7.98%; N, 5.69%. Found: C, 69.06%; H, 7.82%; N, 5.40%.

Preparation of $[(\text{IPr})\text{Ni}(\mu\text{-I})]_2$ (6). Following the procedure used to form $[(\text{IPr})\text{Ni}(\mu\text{-Cl})]_2$, 33.0 mg (0.105 mmol) of NiI_2 , 29.0 mg (0.105 mmol) of $\text{Ni}(\text{COD})_2$, 82.0 mg of IPr (0.211 mmol), and 4 mL of toluene were added to a 20 mL scintillation vial. The reaction was allowed to stir for 18 h. The reaction solution was then filtered, and the solvent was removed under reduced pressure. The resulting crude solid was dissolved in minimal toluene, layered with pentane, and cooled to -35°C for 18 h to obtain 75.4 mg (62%) of black/yellow crystals of 6. ^1H NMR (600.13 MHz, C_6D_6): δ 7.21 (t, J = 7.70 Hz, 4H, para-CH), 7.13 (d, J = 7.64 Hz, 8H, meta-CH), 6.13 (s, 4H, NCH), 3.20 (m, J = 6.85 Hz, 8H, $\text{CH}(\text{CH}_3)_2$), 2.26 (d, J = 6.84 Hz, 24H, $\text{CH}(\text{CH}_3)_2$), 1.05 (d, J = 6.90 Hz, 24H, $\text{CH}(\text{CH}_3)_2$). $^{13}\text{C}\{\text{H}\}$ NMR (150.92 MHz, C_6D_6): δ 178.06 (carbene C), 145.95, 137.18, 129.53 (NCH), 124.08, 123.59, 29.04 ($\text{CH}(\text{CH}_3)_2$), 25.11 (CH- $\text{CH}_3)_2$), 24.96 ($\text{CH}(\text{CH}_3)_2$). Anal. Calcd for $\text{C}_{54}\text{H}_{72}\text{N}_4\text{I}_2\text{Ni}_2$: C, 56.48%; H, 6.32%; N, 4.88%. Found: C, 56.77%; H, 6.23%; N, 4.71%.

Computational Details. All calculations were performed using Gaussian 16 (revision A03)⁴¹ on the Tiger cluster at UC Berkeley Molecular Graphics and Computing Facility. Geometry optimizations for 1 were performed from coordinates taken from the corresponding crystal structure. Calculations for 1 were performed using the def2-TZVP basis set for Ni and the atoms directly bonded to Ni, while def2-svpp was used for all other atoms.⁴⁴ The PBE0-D3 functional was used for these calculations.

ASSOCIATED CONTENT

Supporting Information

The Supporting Information is available free of charge at <https://pubs.acs.org/doi/10.1021/acs.organomet.2c00188>.

DFT files (ZIP)

Solid state structure figures and data tables and NMR spectra of $[(\text{IPr})\text{Ni}(\mu\text{-CH}_3)]_2$ (1), $[(\text{IPr})\text{Ni}(\mu\text{-SiH}_3)]_2$ (2), $[(\text{IPr})\text{Ni}(\text{CH}_3)]_2\text{CO}_3$ (3), and $[(\text{IPr})\text{Ni}(\mu\text{-I})]_2$ (6) (PDF)

Accession Codes

CCDC 2165566–2165569 contain the supplementary crystallographic data for this paper. These data can be obtained free of charge via www.ccdc.cam.ac.uk/data_request/cif, or by emailing data_request@ccdc.cam.ac.uk, or by contacting The Cambridge Crystallographic Data Centre, 12 Union Road, Cambridge CB2 1EZ, UK; fax: +44 1223 336033.

AUTHOR INFORMATION

Corresponding Author

T. Don Tilley – Department of Chemistry, University of California Berkeley, Berkeley, California 94720, United States; Chemical Sciences Division, Lawrence Berkeley National Laboratory, Berkeley, California 94720, United States; orcid.org/0000-0002-6671-9099; Email: tdtilley@berkeley.edu

Author

Ryan J. Witzke – Department of Chemistry, University of California Berkeley, Berkeley, California 94720, United States; Chemical Sciences Division, Lawrence Berkeley National Laboratory, Berkeley, California 94720, United States; Present Address: Sandia National Laboratories, Livermore, California 94550, United States; orcid.org/0000-0003-1729-1636

Complete contact information is available at:

<https://pubs.acs.org/doi/10.1021/acs.organomet.2c00188>

Notes

The authors declare no competing financial interest.

ACKNOWLEDGMENTS

We thank the National Science Foundation for their support of this work under grant no. CHE-1954808. X-ray analysis of **1**, **2**, **3**, and **6** used resources of the ALS, which is a DOE Office of Science User Facility under contract no. DE-AC02-05CH11231. We acknowledge the NIH (grant nos. SRR023679A and 1S10RR016634-01) and NSF (grant no. CHE-0130862) for funding of the College of Chemistry NMR facility (UC, Berkeley).

REFERENCES

(1) Bellucci, I.; Corelli, R. Verbindungen Des Einwertigen Nickels. *Z. Anorg. Chem.* **1914**, *86*, 88–104.

(2) Lin, C.-Y.; Power, P. P. Complexes of Ni(I): A “Rare” Oxidation State of Growing Importance. *Chem. Soc. Rev.* **2017**, *46*, 5347–5399.

(3) Bismuto, A.; Finkelstein, P.; Müller, P.; Morandi, B. The Journey of Ni(I) Chemistry. *Helv. Chim. Acta* **2021**, *104*, No. e2100177.

(4) Zimmermann, P.; Limberg, C. Activation of Small Molecules at Nickel(I) Moieties. *J. Am. Chem. Soc.* **2017**, *139*, 4233–4242.

(5) Grabarse, W.; Mahlert, F.; Duin, E. C.; Goubeaud, M.; Shima, S.; Thauer, R. K.; Lamzin, V.; Ermler, U. On the Mechanism of Biological Methane Formation: Structural Evidence for Conformational Changes in Methyl-Coenzyme M Reductase upon Substrate Binding. *J. Mol. Biol.* **2001**, *309*, 315–30.

(6) Volbeda, A.; Amara, P.; Darnault, C.; Mouesca, J.-M.; Parkin, A.; Roessler, M. M.; Armstrong, F. A.; Fontecilla-Camps, J. C. X-Ray Crystallographic and Computational Studies of the O₂-Tolerant [NiFe]-Hydrogenase 1 from Escherichia Coli. *Proc. Natl. Acad. Sci. U.S.A.* **2012**, *109*, 5305–5310.

(7) Darnault, C.; Volbeda, A.; Kim, E. J.; Legrand, P.; Vernède, X.; Lindahl, P. A.; Fontecilla-Camps, J. C. Ni-Zn-[Fe₄S₄] and Ni-Ni-[Fe₄S₄] Clusters in Closed and Open α Subunits of Acetyl-CoA Synthase/Carbon Monoxide Dehydrogenase. *Nat. Struct. Biol.* **2003**, *10*, 271–279.

(8) Han, F.-S. Transition-Metal-Catalyzed Suzuki-Miyaura Cross-Coupling Reactions: A Remarkable Advance from Palladium to Nickel Catalysts. *Chem. Soc. Rev.* **2013**, *42*, 5270–5298.

(9) Tasker, S. Z.; Standley, E. A.; Jamison, T. F. Recent Advances in Homogeneous Nickel Catalysis. *Nature* **2014**, *509*, 299–309.

(10) Ananikov, V. P. Nickel: The “Spirited Horse” of Transition Metal Catalysis. *ACS Catal.* **2015**, *5*, 1964–1971.

(11) Hazari, N.; Melvin, P. R.; Beromi, M. M. Well-Defined Nickel and Palladium Precatalysts for Cross-Coupling. *Nat. Rev. Chem.* **2017**, *1*, 0025.

(12) Lipschutz, M. I.; Tilley, T. D. Carbon-Carbon Cross-Coupling Reactions Catalyzed by a Two-Coordinate Nickel(II)-Bis(Amido) Complex via Observable NiI, NiII, and NiIII Intermediates. *Angew. Chem., Int. Ed.* **2014**, *53*, 7290–7294.

(13) Matsubara, K.; Yamamoto, H.; Miyazaki, S.; Inatomi, T.; Nonaka, K.; Koga, Y.; Yamada, Y.; Veiro, L. F.; Kirchner, K. Dinuclear Systems in the Efficient Nickel-Catalyzed Kumada-Tamao-Corriu Cross-Coupling of Aryl Halides. *Organometallics* **2017**, *36*, 255–265.

(14) Yin, H.; Fu, G. C. Mechanistic Investigation of Enantioconvergent Kumada Reactions of Racemic α -Bromoketones Catalyzed by a Nickel/Bis(Oxazoline) Complex. *J. Am. Chem. Soc.* **2019**, *141*, 15433–15440.

(15) Anderson, T. J.; Jones, G. D.; Vicic, D. A. Evidence for a Ni Active Species in the Catalytic Cross-Coupling of Alkyl Electrophiles. *J. Am. Chem. Soc.* **2004**, *126*, 8100–8101.

(16) Jones, G. D.; Martin, J. L.; McFarland, C.; Allen, O. R.; Hall, R. E.; Haley, A. D.; Brandon, R. J.; Konovalova, T.; Desrochers, P. J.; Pulay, P.; Vicic, D. a. Ligand Redox Effects in the Synthesis, Electronic Structure, and Reactivity of an Alkyl-Alkyl Cross-Coupling Catalyst. *J. Am. Chem. Soc.* **2006**, *128*, 13175–13183.

(17) Diccianni, J. B.; Hu, C. T.; Diao, T. Insertion of CO₂ Mediated by a (Xantphos)Ni I -Alkyl Species. *Angew. Chem., Int. Ed.* **2019**, *58*, 13865–13868.

(18) Dible, B. R.; Sigman, M. S.; Arif, A. M. Oxygen-Induced Ligand Dehydrogenation of a Planar Bis- μ -Chloronickel(I) Dimer Featuring an NHC Ligand. *Inorg. Chem.* **2005**, *44*, 3774–3776.

(19) Laskowski, C. A.; Bungum, D. J.; Baldwin, S. M.; Del Ciello, S. A.; Iluc, V. M.; Hillhouse, G. L. Synthesis and Reactivity of Two-Coordinate Ni(I) Alkyl and Aryl Complexes. *J. Am. Chem. Soc.* **2013**, *135*, 18272–18275.

(20) Witzke, R. J.; Tilley, T. D. A Two-Coordinate Ni(I) Silyl Complex: CO₂ Insertion and Oxidatively-Induced Silyl Migrations. *Chem. Commun.* **2019**, *55*, 6559–6562.

(21) Laskowski, C. A.; Hillhouse, G. L. Two-Coordinate d9 Complexes. Synthesis and Oxidation of NHC Nickel (I) Amides. *J. Am. Chem. Soc.* **2008**, *130*, 13846–13847.

(22) Krüger, C.; Sekutowski, J. C.; Berke, H.; Hoffmann, R. Struktur Und Bindungsverhältnisse Eines Alkyl-Verbrückten Ni-Ni-Systems The Bonding in an Alkyl-Bridged Ni-Ni System. *Z. Naturforsch.* **1978**, *33*, 1110–1115.

(23) Pauling, L. Atomic Radii and Interatomic Distances in Metals. *J. Am. Chem. Soc.* **1947**, *69*, 542–553.

(24) Walsh, R. Bond Dissociation Energy Values in Silicon-Containing Compounds and Some of Their Implications. *Acc. Chem. Res.* **1981**, *14*, 246–252.

(25) Iluc, V. M.; Hillhouse, G. L. Arrested 1,2-Hydrogen Migration from Silicon to Nickel upon Oxidation of a Three-Coordinate Ni(I) Silyl Complex. *J. Am. Chem. Soc.* **2010**, *132*, 11890–11892.

(26) Handford, R. C.; Smith, P. W.; Tilley, T. D. Silylene Complexes of Late 3d Transition Metals Supported by Tris-Phosphinoborate Ligands. *Organometallics* **2018**, *37*, 4077–4085.

(27) Waterman, R.; Hayes, P. G.; Tilley, T. D. Synthetic Development and Chemical Reactivity of Transition-Metal Silylene Complexes. *Acc. Chem. Res.* **2007**, *40*, 712–719.

(28) Lee, C. H.; Laitar, D. S.; Mueller, P.; Sadighi, J. P. Generation of a Doubly Bridging CO₂ Ligand and Deoxygenation of CO₂ by an (NHC)Ni(0) Complex. *J. Am. Chem. Soc.* **2007**, *129*, 13802–13803.

(29) Aresta, M.; Dibenedetto, A. Utilisation of CO₂ as a Chemical Feedstock: Opportunities and Challenges. *Dalton Trans.* **2007**, *28*, 2975–2992.

(30) Beller, M.; Bornscheuer, U. T. CO₂ fixation through Hydrogenation by Chemical or Enzymatic Methods. *Angew. Chem., Int. Ed.* **2014**, *53*, 4527–4528.

(31) Horn, B.; Limberg, C.; Herwig, C.; Braun, B. Nickel(I)-Mediated Transformations of Carbon Dioxide in Closed Synthetic Cycles: Reductive Cleavage and Coupling of CO₂ Generating Ni^ICO, Ni^{II}CO₃ and Ni^{II}C₂O₄Ni^{II} Entities. *Chem. Commun.* **2013**, *49*, 10923–10925.

(32) Vollmer, M. V.; Cammarota, R. C.; Lu, C. C. Reductive Disproportionation of CO₂ Mediated by Bimetallic Nickelate(-I)/Group 13 Complexes. *Eur. J. Inorg. Chem.* **2019**, *2019*, 2140–2145.

(33) Zimmermann, P.; Kilpatrick, A. F. R.; Ar, D.; Demeshko, S.; Cula, B.; Limberg, C. Electron Transfer within β -Diketiminato Nickel Bromide and Cobaltocene Redox Couples Activating CO₂. *Chem. Commun.* **2021**, *57*, 875–878.

(34) Dorta, R.; Stevens, E. D.; Scott, N. M.; Costabile, C.; Cavallo, L.; Hoff, C. D.; Nolan, S. P. Steric and Electronic Properties of N-Heterocyclic Carbenes (NHC): A Detailed Study on Their Interaction with Ni(CO)₄. *J. Am. Chem. Soc.* **2005**, *127*, 2485–2495.

(35) Lipschutz, M. I.; Tilley, T. D. Useful Method for the Preparation of Low-Coordinate Nickel(I) Complexes via Transformations of the Ni(I) Bis(Amido) Complex K{Ni[N(SiMe₃)(2,6-(i)Pr₂-C₆H₃)]₂}. *Organometallics* **2014**, *33*, 5566–5570.

(36) Zhang, K.; Conda-Sheridan, M.; Cooke, S.; Louie, J. N-Heterocyclic Carbene Bound Nickel (I) Complexes and Their Roles in Catalysis. *Organometallics* **2011**, *30*, 2546–2552.

(37) Tilley, T. D. Transition-Metal Silyl Derivatives. In *The Chemistry of Organic Silicon Compounds*; Patai, S., Rappoport, Z., Eds.; Wiley & Sons: New York, 1989; pp 1415–1477.

(38) Tilley, T. D. The Silicon-Heteroatom Bond. In *The Silicon-Heteroatom Bond*; Patai, S., Rappoport, Z., Eds.; Wiley & Sons: New York, 1991; pp 245–308.

(39) Evans, D. F. The Determination of the Paramagnetic Susceptibility of Substances by NMR. *J. Chem. Soc.* **1959**, 2003–2005.

(40) Sheldrick, G. M. Crystal Structure Refinement with SHELXL. *Acta Crystallogr., Sect. C: Struct. Chem.* **2015**, *71*, 3–8.

(41) Sheldrick, G. M. SHELXT - Integrated Space-Group and Crystal-Structure Determination. *Acta Crystallogr., Sect. A: Found. Adv.* **2015**, *71*, 3–8.

(42) Sheldrick, G. M. Short History of SHELX. *Acta Crystallogr., Sect. A: Found. Adv.* **2008**, *64*, 112–122.

(43) Dolomanov, O. V.; Bourhis, L. J.; Gildea, R. J.; Howard, J. A. K.; Puschmann, H. OLEX2: A Complete Structure Solution, Refinement and Analysis Program. *J. Appl. Crystallogr.* **2009**, *42*, 339–341.

(44) Weigend, F.; Ahlrichs, R. Balanced Basis Sets of Split Valence, Triple Zeta Valence and Quadruple Zeta Valence Quality for H to Rn: Design and Assessment of Accuracy. *Phys. Chem. Chem. Phys.* **2005**, *7*, 3297–3305.

□ Recommended by ACS

Synthesis of Terminal Bis(hydrosulfido) and Disulfido Complexes of Ni(II) from a Geometrically Frustrated Tetrahedral Ni(II) Chloride Complex

Tobias J. Sherbow, Michael D. Pluth, *et al.*

MAY 17, 2021

INORGANIC CHEMISTRY

READ ▶

Ni(4-tBustb)3: A Robust 16-Electron Ni(0) Olefin Complex for Catalysis

Lukas Nattmann and Josep Cornella

SEPTEMBER 10, 2020

ORGANOMETALLICS

READ ▶

Generation of a Ni3 Phosphinidene Cluster from the Ni(0) Synthon, Ni(η 3-CPh3)2

Alexander J. Touchton, Trevor W. Hayton, *et al.*

APRIL 07, 2020

ORGANOMETALLICS

READ ▶

Nickel(II)-SNS Thiolate Complexes: Reactivity and Solution Dynamics

Yahya M. Albkuri, R. Tom Baker, *et al.*

JULY 09, 2021

INORGANIC CHEMISTRY

READ ▶

Get More Suggestions >